Research Square

Preprints are preliminary reports that have not undergone peer review.
They should not be considered conclusive, used to inform clinical practice,
or referenced by the media as validated information.

# Development and Validation of an MRI-Based Nomogram for Risk Stratification of Anxiety in Parkinson's Disease

**Huizhen Wang**

2485202411@qq.com

The Central Hospital of Enshi Tujia and Miao Autonomous Prefecture

**Shijun Yang**

The Central Hospital of Enshi Tujia and Miao Autonomous Prefecture

**Bowen Wang**

The Central Hospital of Enshi Tujia and Miao Autonomous Prefecture

**Jinhai Liu**

The Central Hospital of Enshi Tujia and Miao Autonomous Prefecture

**Congping Wang**

The Central Hospital of Enshi Tujia and Miao Autonomous Prefecture

**Qunhui Liu**

The Central Hospital of Enshi Tujia and Miao Autonomous Prefecture

**Ling Ran**

The Lichuan Second People's Hospital

**Min Jia**

The Central Hospital of Enshi Tujia and Miao Autonomous Prefecture

**Research Article**

**Keywords:** Parkinson's disease, anxiety, structural MRI, nomogram, predictive model

**Posted Date:** November 5th, 2026

**DOI:** https://doi.org/10.21203/rs.3.rs-10893516/v1

**License:** This work is licensed under a Creative Commons Attribution 4.0 International License.
Read Full License

**Additional Declarations:** No competing interests reported.

## Abstract

# Objective

Anxiety, a common and disabling non-motor symptom of Parkinson's disease (PD), highlights the clinical importance of early identification of PD with anxiety (PDA). This study aimed to develop and internally validate an nomogram that integrates routine clinical indicators and structural MRI radiomic features for early PDA risk stratification.

# Methods

139 PD patients were retrospectively enrolled and split into training (n = 97) and internal test (n = 42) sets at a 7:3 ratio. 21 clinical variables were collected, and 584 quantitative morphological features were extracted. Mann-Whitney U test, Spearman collinearity elimination and least absolute shrinkage and selection operator (LASSO) regression were used to select optimal imaging metrics to calculate a radiomics signature. Univariate and multivariate logistic regression identified independent clinical predictors. A clinical prediction model and an integrated clinical–radiomics nomogram were constructed, and assessed in terms of accuracy, sensitivity, specificity, precision, positive predictive value, negative predictive value, F1-score, receiver-operating characteristic (ROC) curves, calibration plots and decision curve analysis (DCA).

# Results

Elevated UPDRS-III score, cognitive impairment, higher levodopa-benserazide dosage, and 12 MRI features were independent PDA predictors. The combined nomogram outperformed the clinical-only model, achieving an AUC of 0.99, accuracy of 0.93, sensitivity of 1.00, specificity of 0.91 in the test set. Calibration curves confirmed favorable consistency between predicted and actual anxiety risk, while DCA demonstrated sustained net clinical benefit of the integrated nomogram across wide threshold ranges.

# Conclusion

The visualizable clinical-radiomics nomogram enables accurate individualized PDA risk prediction. This non-invasive, bedside-accessible tool assists neurologists in early screening and stratified management of PDA.

## 1. Introduction

Parkinson's disease (PD) is recognized as the second most prevalent neurodegenerative disorder associated with aging, with an estimated prevalence of approximately 3% among individuals aged 65 years and above[1]. Clinically, PD is characterized not only by its hallmark motor manifestations, such as

resting tremor, bradykinesia, muscular rigidity, and impaired postural control, but also by a wide spectrum of non-motor symptoms that substantially contribute to disease burden[2, 3].Anxiety is one of the most common and disabling non-motor symptoms, with a reported prevalence of approximately 40% [4]. Anxiety in patients with PD is associated with several adverse clinical outcomes, including faster disease progression, greater motor impairment, reduced responsiveness to levodopa, an increased risk of treatment-related adverse events, poorer quality of life independent of motor severity, and higher mortality[5–8]. Despite these substantial clinical consequences, the neuroimaging mechanisms underlying Parkinson's disease with anxiety (PDA) remain poorly understood. Moreover, no quantitative imaging biomarkers of structural brain changes are currently available for clinical use.

Among currently available multimodal magnetic resonance imaging (MRI) approaches, structural MRI (sMRI) provides intuitive, reliable, and robust measures and has therefore been widely used in studies of neurodegenerative diseases. Analytical approaches for sMRI include voxel-based morphometry (VBM), surface-based morphometry (SBM), and fine-grained brain parcellation. Both VBM and SBM enable objective characterization of structural changes in the central nervous system, providing insights into disease pathophysiology and supporting diagnostic and prognostic assessments. VBM quantifies gray matter volume (GMV) and white matter volume (WMV) at the voxel level, allowing sensitive detection of regional morphological changes. SBM involves brain tissue segmentation and cortical reconstruction to derive quantitative measures of gray matter morphology, including cortical thickness, local gyrification index (GI), fractal dimension (FD), and sulcal depth. In PD, *α*-synuclein pathology may affect the amygdala before the onset of motor symptoms and disrupt its functional connectivity with the hippocampus. Such disruption may impair emotional memory and enhance negative thinking, thereby contributing to the development of anxiety[9]. Therefore, precise subregional segmentation of the hippocampus and amygdala is important for elucidating the neuroanatomical basis of PDA and identifying potential imaging biomarkers for early detection. VBM, SBM, hippocampal subfield segmentation, and amygdala subnuclei parcellation are complementary approaches that may improve the sensitivity and specificity of sMRI for characterizing neuroanatomical changes in neuropsychiatric disorders, including Alzheimer's disease (AD) and PD[10].

In the present study, we systematically evaluated a range of neuroimaging metrics based on VBM, SBM, and fine-grained parcellation of the hippocampus and amygdala to identify imaging features associated with PDA. We then developed and internally validated a practical and interpretable nomogram that integrates routine clinical variables for individualized risk estimation[11, 12]. This approach translates advanced computational methods into clinically applicable risk scores. It may help neurologists identify patients with PD who are at high risk of anxiety during the early stage of the disease and support risk-stratified management and targeted interventions.

## 2. Materials and methods

## 2.1 Study population

In this retrospective investigation, consecutive patients with a confirmed diagnosis of PD who underwent evaluation and treatment at The Central Hospital of Enshi Tujia and Miao Autonomous Prefecture between July 2018 and December 2025 were included. Eligibility for study participation was determined according to the following inclusion criteria: (1) idiopathic PD diagnosed according to the UK Brain Bank criteria[13]; (2) complete medical records and documented dates of scale assessments; and (3) completion of neurological examination and sMRI scanning. The exclusion criteria were as follows: (1) coexisting neurological disorders, such as epilepsy, stroke, intracranial neoplasms, or multiple sclerosis; (2) a history of intracranial space-occupying lesions, craniotomy, or traumatic brain injury; (3) a history of alcohol or substance abuse; (4) use of anxiolytic agents within 30 days before treatment initiation; and (5) severe cardiovascular, hepatic, or renal dysfunction. Anxiety was evaluated with the Parkinson Anxiety Scale (PAS)[14]. According to the predefined cutoff value, participants with a PAS total score of ≥ 14 were categorized as having anxiety, whereas those with scores below 14 were classified as having no anxiety. The study protocol received approval from the Institutional Review Board of The Central Hospital of Enshi Tujia and Miao Autonomous Prefecture (approval No. 2026-006-01). All participants provided written informed consent before enrollment.

## 2.2 Clinical information

Baseline clinical data were collected from each participant, including sex, years of education, smoking status, alcohol consumption, hypertension, diabetes mellitus, dysautonomia, hyperlipidemia, age, age at disease onset, PD duration, Unified Parkinson's Disease Rating Scale Part III (UPDRS-III) score, Unified Parkinson's Disease Rating Scale Part IV (UPDRS-IV) score, Hoehn–Yahr (H-Y) stage, cognitive impairment (MoCA score < 24), sleep disorder, and symptom onset side (left, right, or bilateral). Medication-related variables included the daily dose of levodopa–benserazide and levodopa-equivalent daily dose (LEDD). Laboratory biomarkers included C-reactive protein (CRP) and serum uric acid levels. In total, 21 clinical features were analyzed.

## 2.3 Image acquisition

All participants underwent brain MRI on the same 3.0-T scanner (Magnetom Verio) at the Department of Radiology of our hospital. High-resolution T1-weighted images were acquired using a combined head and neck coil. The three-dimensional T1-weighted magnetization-prepared rapid gradient-echo (3D-T1-MPRAGE) sequence was performed with the following parameters: repetition time (TR) = 2300 ms, inversion time (TI) = 900 ms, echo time (TE) = 2.01 ms, flip angle = 8°, voxel size = 1.0 × 1.0 × 1.0 mm, 176 slices with a slice thickness of 1.0 mm and a slice gap of 1.0 mm, field of view (FOV) = 250 × 100 mm, and matrix size = 256 × 256.

## 2.4 Radiomics feature segmentation and extraction

Structural T1-weighted MRI scans were processed using FreeSurfer (version 7.4.1, https://surfer.nmr.mgh.harvard.edu/). The standard recon-all pipeline was used for skull stripping, tissue segmentation, cortical surface reconstruction, and subregional parcellation. A range of quantitative imaging features was automatically extracted, including VBM-derived volumes of gray matter, white

matter, and multiple subcortical structures; SBM metrics, including cortical thickness, intrinsic curvature index, local gyrification index, Gaussian curvature, and mean curvature; hippocampal subfield volumes; and amygdala subnuclear volumes. Additional features included volumetric measures of the ventricular system, cerebellar structures, brainstem, cerebrospinal fluid, individual segments of the corpus callosum, white matter hyperintensities, and whole-brain structures, as well as cortical topology quality-control indices. Two radiologists independently performed the segmentation while blinded to the patients' clinical diagnoses. Kappa consistency analysis was used to assess inter-rater agreement, with a Kappa value ≥ 0.85 considered indicative of good agreement. All imaging metrics obtained from FreeSurfer were exported for subsequent statistical analysis and predictive model development.

## 2.5 Radiomics feature selection

Prior to feature selection, all manually derived radiomic variables were standardized using Z-score transformation to minimize the influence of differences in measurement scales. The subsequent screening process consisted of three sequential procedures. Initially, the Mann–Whitney U test was applied to each candidate feature for preliminary discrimination, and only variables reaching statistical significance ($P < 0.05$) were carried forward. The retained features were then subjected to Spearman rank correlation analysis to evaluate correlations between variables and identify redundant features arising from potential multicollinearity. When the absolute correlation coefficient exceeded 0.9, one of the highly correlated features was removed. Finally, LASSO regression was used to identify the most relevant predictors for model development. A composite radiomic score (Rad-score) was subsequently calculated based on the coefficients of the selected features. Ten-fold cross-validation was used during LASSO model development to determine the optimal feature set.

## 2.6 Model development and validation

The entire cohort was randomly divided into a training set and an internal test set at a ratio of 7:3. Two predictive models were developed using the training set: Model I, a clinical-only model, and Model II, a combined clinical–radiomics model. To enhance clinical applicability, Model II was presented as a nomogram. Both predictive models were subsequently validated using the internal test cohort. Their classification performance was characterized by several complementary metrics, including accuracy, sensitivity, specificity, precision, positive predictive value (PPV), negative predictive value (NPV), and F1-score. Discriminative ability was further examined by constructing ROC curves and determining the corresponding AUC. Model calibration was evaluated by comparing the probabilities estimated by the models with the actual proportions of observed outcomes. Finally, DCA was conducted across a range of threshold probabilities to quantify the net benefit and assess the potential clinical usefulness of each predictive model.

## 2.7 Statistical analysis

Statistical analyses were conducted with Python using the scikit-learn package (version 0.13.2). For continuous data, between-group differences were evaluated with either the Student's *t*-test or the Mann–Whitney U test according to the underlying data distribution. Categorical variables were analyzed using

the $\chi^2$ test or Fisher's exact test, as appropriate. Continuous variables following a normal distribution are reported as mean ± standard deviation (SD), whereas skewed data are summarized as median values with interquartile ranges (IQRs). Logistic regression models were used to estimate odds ratios (ORs) together with their corresponding 95% confidence intervals (CIs). Initially, univariate logistic regression was conducted to screen potential predictors, and variables with $P < 0.30$ were considered eligible for subsequent multivariable analysis. Multivariate logistic regression was subsequently performed to determine the independent predictors included in the final model. Unless otherwise indicated, a two-sided $P$ value < 0.05 was regarded as statistically significant.

# 3. Results

## 3.1 Clinical and demographic characteristics

A total of 139 patients with PD were included in the final analysis. These participants were randomly allocated to a training cohort of 97 patients, consisting of 34 individuals with anxiety and 63 without anxiety, and an internal test cohort of 42 patients, comprising 10 individuals with anxiety and 32 without anxiety. Comparison of baseline demographic and clinical characteristics between the two cohorts revealed no statistically significant differences across the evaluated variables ($P > 0.05$), suggesting that the two cohorts were well balanced and had similar baseline characteristics. The baseline demographic and clinical characteristics of the subgroups are summarized in Table 1. Multivariate logistic regression analysis identified UPDRS-III score ($P = 0.041$; OR = 1.030, 95% CI: 1.000–1.052), cognitive impairment ($P = 0.014$; OR = 1.094, 95% CI: 1.021–1.163), and levodopa–benserazide dosage ($P < 0.001$; OR = 1.010, 95% CI: 1.005–1.014) as independent predictors of PDA (Table 2).

Table 1
Clinical and demographic characteristics.

| Variables | Overall (n = 139) | PD without anxiety(n = 95) | PD with anxiety(n = 44) | *P* |
|---|---|---|---|---|
| Gender (%) | | | | 0.796 |
| Women | 72 (51.80) | 48 (50.53) | 24 (54.55) | |
| Man | 67 (48.20) | 47 (49.47) | 20 (45.45) | |
| Education * | 6.00 (6.00, 9.00) | 6.00 (6.00, 9.00) | 6.00 (6.00, 9.00) | 0.926 |
| Smoking (%) | | | | 0.312 |
| No | 115 (82.73) | 76 (80.00) | 39 (88.64) | |
| Yes | 24 (17.27) | 19 (20.00) | 5 (11.36) | |
| Drinking (%) | | | | 0.042 |
| No | 123 (88.49) | 80 (84.21) | 43 (97.73) | |
| Yes | 16 (11.51) | 15 (15.79) | 1 (2.27) | |
| Hypertension (%) | | | | 0.518 |
| No | 86 (61.87) | 61 (64.21) | 25 (56.82) | |
| Yes | 53 (38.13) | 34 (35.79) | 19 (43.18) | |
| Diabetes (%) | | | | 0.796 |
| No | 130 (93.53) | 88 (92.63) | 42 (95.45) | |
| Yes | 9 (6.47) | 7 (7.37) | 2 (4.55) | |
| Dysautonomia (%) | | | | 0.736 |
| No | 99 (71.22) | 69 (72.63) | 30 (68.18) | |
| Yes | 40 (28.78) | 26 (27.37) | 14 (31.82) | |
| Hyperlipidemia (%) | | | | 0.772 |
| No | 94 (67.63) | 63 (66.32) | 31 (70.45) | |
| Yes | 45 (32.37) | 32 (33.68) | 13 (29.55) | |
| CRP * | 0.81 (0.31, 2.30) | 0.68 (0.28, 1.90) | 1.34 (0.54, 2.66) | 0.081 |
| Serum urate concentration † | 299.05 (80.96) | 304.36 (85.96) | 287.59 (68.44) | 0.257 |
| *P* < 0.05 was statistically significant. | | | | |

| Variables | Overall (n = 139) | PD without anxiety(n = 95) | PD with anxiety(n = 44) | *P* |
|---|---|---|---|---|
| Age * | 69.00 (61.00, 74.00) | 68.00 (60.00, 73.00) | 69.00 (65.00, 75.25) | 0.192 |
| Age of onset * | 65.00 (57.00, 70.00) | 65.00 (57.00, 70.00) | 65.00 (58.00, 69.25) | 0.767 |
| Duration of PD * | 3.00 (1.00, 5.00) | 2.00 (1.00, 5.00) | 4.50 (2.00, 8.00) | < 0.001 |
| UPDRS Ⅲ score * | 23.00 (15.00, 30.00) | 20.00 (15.00, 28.00) | 30.00 (20.00, 35.00) | 0.001 |
| UPDRS Ⅱ score * | 0.00 (0.00, 2.00) | 0.00 (0.00, 2.00) | 1.00 (0.00, 4.00) | 0.004 |
| Hoehn and Yahr stages * | 2.50 (2.00, 3.00) | 2.00 (2.00, 3.00) | 3.00 (2.50, 4.00) | < 0.001 |
| Cognitive impairment (%) | | | | 0.172 |
| No | 116 (83.45) | 76 (80.00) | 40 (90.91) | |
| Yes | 23 (16.55) | 19 (20.00) | 4 (9.09) | |
| Sleep disorder (%) | | | | 0.182 |
| No | 70 (50.36) | 52 (54.74) | 18 (40.91) | |
| Yes | 69 (49.64) | 43 (45.26) | 26 (59.09) | |
| Symptom onset side (%) | | | | 0.050 |
| Left | 8 (5.76) | 7 (7.37) | 1 (2.27) | |
| Right | 18 (12.95) | 16 (16.84) | 2 (4.55) | |
| Both | 113 (81.29) | 72 (75.79) | 41 (93.18) | |
| Levodopa Benserazide * | 375.00 (218.75, 500.00) | 375.00 (187.50, 375.00) | 500.00 (375.00, 562.50) | < 0.001 |
| LEDD * | 450.00 (262.50, 662.50) | 400.00 (262.50, 468.75) | 694.00 (450.00, 900.00) | < 0.001 |
| *P* < 0.05 was statistically significant. | | | | |

Abbreviations: PD, Parkinson's disease; UPDRS, Unified Parkinson’s Disease Rating Scale; CRP, C reactive protein; LEDD, levodopa equivalent daily dose. *, median (interquartile range, 25th–75th percentiles); †, mean (standard deviation).

Table 2
The univariate and multivariate logistic regression analysis of training set.

| Variables | Univariate logistic regression analysis | | Multivariate logistic regression analysis | |
|---|---|---|---|---|
| | *OR (95%CI)* | *P* | *OR (95%CI)* | *P* |
| Gender | 1.172(0.509–2.702) | 0.709 | | |
| Education | 0.996(0.886–1.119) | 0.946 | | |
| Smoking | 0.663(0.215–2.049) | 0.475 | | |
| Drinking | 0.143(0.018–1.161) | 0.069 | | |
| Hypertension | 1.006(0.426–2.374) | 0.989 | | |
| Diabetes | 0.594(0.113–3.116) | 0.538 | | |
| Dysautonomia | 1.224(0.483–3.104) | 0.670 | | |
| Hyperlipidemia | 1.028(0.421–2.512) | 0.951 | | |
| CRP | 1.083(0.967–1.212) | 0.168 | | |
| Serum urate concentration | 0.999(0.993–1.004) | 0.699 | | |
| Age | 1.016(0.971–1.062) | 0.497 | | |
| Age of onset | 0.991(0.951–1.032) | 0.656 | | |
| Duration of PD | 1.223(1.072–1.395) | 0.003 | | |
| UPDRS Ⅱ score | 1.047(1.009–1.086) | 0.015 | 1.030(1.000-1.052) | 0.041 |
| UPDRS Ⅲ score | 1.300(1.061–1.593) | 0.011 | | |
| Hoehn and Yahr stages | 2.497(1.440–4.331) | 0.001 | | |
| Cognitive impairment | 0.339(0.090–1.275) | 1.094 | 1.094(1.021–1.163) | 0.014 |
| Sleep disorder | 1.393(0.603–3.222) | 0.438 | | |
| Symptom onset side | | | | |
| Left | 1.000 | | | |
| Right | 2845701.966(0-Inf) | 0.991 | | |
| Both | 10221296.859(0-Inf) | 0.991 | | |
| Levodopa Benserazide | 1.008(1.004–1.012) | < 0.001 | 1.010(1.005–1.014) | < 0.001 |
| LEDD | 1.005(1.003–1.007) | < 0.001 | | |

Abbreviations: PD, Parkinson's disease; UPDRS, Unified Parkinson's Disease Rating Scale; CRP, C reactive protein; OR, odds ratio; CI, confidence interval; LEDD, levodopa equivalent daily dose.

## 3.2 Radiomics characteristics

A total of 584 radiomic features were extracted from the sMRI data, including 64 VBM features, 456 SBM features, 20 features from segmented amygdala subregions, and 44 features from segmented hippocampal subfields. The Mann–Whitney U test was first used for preliminary feature screening, retaining 165 features. Spearman correlation analysis was then performed to remove highly collinear features, leaving 97 features with significant between-group differences. LASSO regression with ten-fold cross-validation was subsequently performed using the minimum criterion to determine the optimal lambda (λ) value. The λ value corresponding to the minimum cross-validation error is shown in Figs. 1 and 2. Finally, 12 features were selected for the final model. These included the volumes of the bilateral hippocampi and bilateral hippocampal tails, as well as the cortical thickness of the bilateral supramarginal gyri, bilateral inferior temporal gyri, bilateral inferior parietal lobules, left middle temporal gyrus, and left insula.

## 3.3 Model construction and performance assessment

Two models were developed to predict the risk of PDA. Model 1 (clinical model) was based exclusively on clinical variables. Model 2, an integrated clinical–radiomics nomogram (Fig. 3), incorporated both clinical and radiomic features to improve its potential for clinical application.

In the internal test cohort, the clinical–radiomics nomogram showed a clear improvement in predictive performance compared with the clinical model. The nomogram yielded an accuracy of 0.93, sensitivity of 1.00, specificity of 0.91, PPV of 0.77, NPV of 1.00, and an F1-score of 0.87, with an AUC of 0.99 (Table 3). The corresponding ROC curves for the clinical and clinical–radiomics models in both the training and internal test cohorts are illustrated in Fig. 4, together with their respective AUC values. The calibration curves showed good agreement between predicted and observed outcomes in both sets (Fig. 4). In addition, DCA showed that the clinical–radiomics nomogram provided greater net clinical benefit than the clinical-only model across the evaluated threshold probabilities for predicting PDA (Fig. 4). A net benefit above zero indicates a potential clinical benefit.

Table 3
The performance of clinical model and combined nomogram for predicting PDA.

| Model | Cohort | AUC (95%CI) | ACC | Sen | Spe | PPV | NPV | F1 |
|---|---|---|---|---|---|---|---|---|
| Clinical | Training set | 0.816 (0.731-0.900) | 0.701 | 0.912 | 0.587 | 0.544 | 0.925 | 0.681 |
| | Test set | 0.731 (0.543–0.920) | 0.595 | 0.900 | 0.500 | 0.360 | 0.941 | 0.514 |
| Combined | Training set | 0.997 (0.990-1.000) | 0.990 | 0.971 | 1.000 | 1.000 | 0.984 | 0.985 |
| | Test set | 0.988 (0.964-1.000) | 0.929 | 1.000 | 0.906 | 0.769 | 1.000 | 0.870 |

Abbreviations: PDA, PD with anxiety; AUC, Area under the curve; ACC, Accuracy; Sen, Sensitivity; Spe, Specificity; PPV, Positive predictive value; NPV, Negative predictive value; F1, F1-Score.

# 4. Discussion

In the present study, we systematically extracted multidimensional structural MRI quantitative metrics, including subcortical volumes, cortical morphological parameters, and hippocampal and amygdala subfield volumes. Based on these features, we developed two predictive models for PDA: a clinical-only model and an integrated clinical–radiomics nomogram that incorporated clinical variables and MRI radiomic features. Internal validation showed that the combined clinical–radiomics nomogram had superior discriminative performance, good calibration, and greater net clinical benefit than the clinical-only model. The visualized nomogram enables rapid and individualized risk estimation for PDA and may have potential clinical value in routine neurological practice.

Previous studies have identified several clinical factors associated with anxiety in patients with PD. Longer disease duration, greater motor severity, higher LEDD, dyskinesia, cognitive impairment, sleep disturbances, and autonomic dysfunction have been reported as potential predictors of PDA[15–18]. In our study, multivariate logistic regression analysis further identified higher UPDRS-III scores and higher daily levodopa–benserazide dosage as independent clinical risk factors for PDA in the training cohort, consistent with previous cross-sectional studies[19–21]. Greater motor impairment may increase psychological burden in patients with PD, while higher dopaminergic medication requirements may reflect more advanced neurodegeneration involving limbic circuits, potentially increasing susceptibility to anxiety. However, the clinical-only model showed limited predictive performance in the internal test set (AUC = 0.731). This finding suggests that conventional clinical measures may not adequately capture subtle structural brain changes associated with PDA, highlighting the potential value of imaging-based predictive tools.

Emerging structural neuroimaging studies have identified widespread gray and white matter changes in PDA, mainly involving brain regions within fear and limbic corticostriatothalamocortical circuits,

including the amygdala, anterior cingulate cortex, prefrontal cortex, insula, thalamic subnuclei, and hippocampal subfields[22–26]. Vriend et al. combined FreeSurfer and VBM analyses and reported reduced amygdala volume in patients with PDA[27]. A combined VBM-SBM study also identified widespread cortical structural changes involving the insula, parietal, occipital, and temporal lobes, as well as the hippocampal regions, in patients with Parkinson's disease dementia (PDD)[28]. Park et al. used FreeSurfer-based thalamic nuclei segmentation and found that several thalamic subnuclei were associated with tremor in PD[29]. However, most existing structural neuroimaging studies of PDA have focused on individual imaging metrics, such as VBM or cortical thickness, and comprehensive analyses integrating multiple structural measures remain limited. Previous MRI studies have mainly used VBM or cortical thickness to assess regional atrophy in PDA. Few studies have systematically integrated multiple quantitative features, including subcortical volumes, cortical morphology, and fine-grained hippocampal and amygdala subregional measures. In the present study, we applied a multi-step feature selection strategy involving Mann–Whitney U testing, Spearman correlation analysis, and LASSO regression with ten-fold cross-validation. This process yielded 12 non-redundant radiomic features for construction of a quantitative Rad-score. These features captured variations in cortical morphology and subcortical volumes and provided additional predictive value beyond clinical variables.

The three independent clinical predictors included in our nomogram UPDRS-III score, cognitive impairment, and levodopa–benserazide dosage are consistent with established clinical risk factors for PDA. A higher UPDRS-III score independently predicted anxiety risk (OR = 1.030, $P = 0.041$), consistent with meta-analytic evidence that greater motor impairment is associated with anxiety in patients with PD[4, 15]. Severe rigidity and bradykinesia can limit daily activities and increase psychological stress. This association is further supported by longitudinal data showing a positive relationship between motor severity and PAS scores[30]. A bidirectional association between cognitive impairment and anxiety was reported in a longitudinal cohort of 368 adults aged ≥ 65 years. Cognitive impairment may contribute to anxiety, while anxiety may further accelerate cognitive decline[31]. One possible explanation is that cognitive impairment may increase anxiety by affecting the regulation of negative emotional memories within the amygdala–hippocampal circuit. Higher levodopa–benserazide dosage was the strongest clinical predictor ($P < 0.001$). This finding is consistent with previous evidence suggesting dose-dependent monoamine imbalance within limbic cortico-striato-thalamo-cortical (CSTC) circuits[27]. Together, these three predictors reflect motor severity, cognitive function, and dopaminergic exposure.

The 12 radiomic signatures condensed into the Rad-score delivered prominent incremental predictive gains when combined with clinical variables, comprising bilateral whole-hippocampus volume, hippocampal tail subfield volume, and DKT-atlas-based cortical thickness metrics covering the insula, supramarginal, inferior parietal, middle temporal, and inferior temporal regions derived from FreeSurfer segmentation. Hippocampal and hippocampal tail subfield indices are consistent with prior FreeSurfer-VBM findings documenting limbic-structure atrophy among PD patients with anxiety, with the hippocampal tail being particularly vulnerable to synuclein-related neurodegeneration[27]. Multiple multimodal MRI studies have highlighted insular and temporoparietal cortical thinning as key morphological alterations in PDA, and surface-based thickness measurements capture subtle

microstructural cortical changes that are invisible to routine visual MRI assessment[22]. The standardized FreeSurfer-DKT segmentation workflow guarantees the reproducibility of these multi-step-screened imaging features for further external validation[32]. The dramatic AUC elevation from the clinical-only model (0.731) to the integrated nomogram (0.988) demonstrated that multidimensional structural morphometric signatures capture silent neurodegenerative alterations missed by conventional clinical evaluation, enabling precise individualized PDA risk stratification at the bedside.

There are several limitations to this study. First, its retrospective, single-center design and relatively small sample size may have introduced selection bias and limited the generalizability of the findings. Larger prospective multicenter cohorts are needed to externally validate the robustness of the model. Second, only structural MRI sequences were included in the current analysis. Future studies could incorporate T2-FLAIR, diffusion tensor imaging, and resting-state functional MRI to assess additional microstructural and functional connectivity features. Finally, serum, cerebrospinal fluid, and electrophysiological biomarkers were not included. Future studies integrating peripheral inflammatory markers and electroencephalographic features may further improve predictive performance.

# 5. Conclusion

In the present study, we identified clinical and limbic morphological features and developed and internally validated a combined clinical–radiomics nomogram for predicting anxiety in patients with Parkinson's disease. The visual nomogram enables individualized risk stratification for PDA and may facilitate early targeted intervention.

# Declarations

**Data availability statement**

The datasets generated and analyzed during the current study are not publicly available due to restrictions imposed by the Ethics Committee of Tujia and Miao Autonomous Prefecture Central Hospital, Enshi, China. However, the data may be made available upon reasonable request to the corresponding author, subject to the applicable ethical and institutional requirements.

**Ethics statement**

Ethical approval for this study was granted by the Ethics Committee of the Central Hospital of Enshi Prefecture (approval No. 2026-006-01). All study procedures were carried out in compliance with applicable local regulations and the relevant institutional requirements. Written informed consent for participation was obtained from the legal guardians or next of kin of all participants.

**Clinical trial number**

Clinical trial number is not applicable.

**Funding**

This work was supported by the General Project of Health Commission of Hubei Province (WJ2025M077).

**Conflicts of interest**

The authors declare that they have no conflict of interest.

**Declaration of Generative AI and AI-assisted Technologies in the Writing Process**

Generative AI and AI-assisted technologies were NOT used in the preparation of this work.

**Acknowledgements**

We gratefully acknowledge all the patients for taking part in this study.

# References

1. Global (2018). *regional, and national burden of Parkinson's disease, 1990–2016: a systematic analysis for the Global Burden of Disease Study 2016*. *Lancet Neurology*, 17(11): pp. 939–953.
2. Jankovic, J. (2008). Parkinson's disease: clinical features and diagnosis. *Journal Of Neurology, Neurosurgery And Psychiatry*, *79*(4), 368–376.
3. Poewe, W., et al. (2017). Parkinson disease. *Nat Rev Dis Primers*, *3*, 17013.
4. Broen, M. P., et al. (2016). Prevalence of anxiety in Parkinson's disease: A systematic review and meta-analysis. *Movement Disorders*, *31*(8), 1125–1133.
5. Lintel, H., et al. (2021). Mood Disorders and Anxiety in Parkinson's Disease: Current Concepts. *J Geriatr Psychiatry Neurol*, *34*(4), 280–288.
6. Hwang, J., et al. (2025). Multidimensional factors of health-related quality of life in parkinson's disease using ensemble learning and network analysis. *Scientific reports*, *15*(1), 36786.
7. Pachana, N. A., et al. (2013). Clinical issues in the treatment of anxiety and depression in older adults with Parkinson's disease. *Movement Disorders*, *28*(14), 1930–1934.
8. Marinus, J., et al. (2018). Risk factors for non-motor symptoms in Parkinson's disease. *Lancet Neurology*, *17*(6), 559–568.
9. Citro, S., et al. (2024). A multiple hits hypothesis for memory dysfunction in Parkinson disease. *Nat Rev Neurol*, *20*(1), 50–61.
10. Wei, X., et al. (2026). Distinct morphological patterns of the hippocampus and amygdala in normal and pathological aging. *Journal Of Alzheimer'S Disease*, *111*(1), 433–453.
11. Li, Z., et al. (2025). Development and validation of a risk stratification model for stroke recurrence after acute ischemic stroke in young adults: A nomogram-based, multicenter retrospective study. *Clinical Neurology And Neurosurgery*, *249*, 108763.

12. Huo, X., et al. (2026). Combinations of clinical factors and radiomics for the hemorrhage-free survival of brainstem cavernous malformation patients. *Clinical Neurology And Neurosurgery*, *262*, 109310.
13. Hughes, A. J., et al. (1992). Accuracy of clinical diagnosis of idiopathic Parkinson's disease: a clinico-pathological study of 100 cases. *Journal Of Neurology, Neurosurgery And Psychiatry*, *55*(3), 181–184.
14. Leentjens, A. F., et al. (2014). The Parkinson Anxiety Scale (PAS): development and validation of a new anxiety scale. *Movement Disorders*, *29*(8), 1035–1043.
15. Sagna, A., Gallo, J. J., & Pontone, G. M. (2014). Systematic review of factors associated with depression and anxiety disorders among older adults with Parkinson's disease. *Parkinsonism & Related Disorders*, *20*(7), 708–715.
16. Wee, N., et al. (2016). Depression and anxiety are co-morbid but dissociable in mild Parkinson's disease: A prospective longitudinal study of patterns and predictors. *Parkinsonism & Related Disorders*, *23*, 50–56.
17. Zhu, K., van Hilten, J. J., & Marinus, J. (2017). Onset and evolution of anxiety in Parkinson's disease. *European Journal Of Neurology*, *24*(2), 404–411.
18. Cui, S. S., et al. (2017). Prevalence and risk factors for depression and anxiety in Chinese patients with Parkinson disease. *Bmc Geriatrics*, *17*(1), 270.
19. Heimrich, K. G., et al. (2024). An examination of anxiety and its influence on health-related quality of life in Parkinson's disease using the geriatric anxiety scale: a cross-sectional study. *Bmc Geriatrics*, *24*(1), 298.
20. Dissanayaka, N. N., et al. (2022). Phenomenology of Atypical Anxiety Disorders in Parkinson's Disease: A Systematic Review. *The American Journal Of Geriatric Psychiatry : Official Journal Of The American Association For Geriatric Psychiatry*, *30*(9), 1026–1050.
21. Upneja, A., et al. (2021). Anxiety in Parkinson's Disease: Correlation with Depression and Quality of Life. *J Neurosci Rural Pract*, *12*(2), 323–328.
22. Carey, G., et al. (2020). Anxiety in Parkinson's disease is associated with changes in the brain fear circuit. *Parkinsonism & related disorders*, *80*, 89–97.
23. Zhang, P., et al. (2022). Regional activity alterations in Parkinson's disease patients with anxiety disorders: A resting-state functional magnetic resonance imaging study. *Frontiers In Aging Neuroscience*, *14*, 1055160.
24. Carey, G., et al. (2023). Cognitive Behavioral Therapy for Anxiety in Parkinson's Disease Induces Functional Brain Changes. *J Parkinsons Dis*, *13*(1), 93–103.
25. Jia, M., et al. (2024). Early identification of Parkinson's disease with anxiety based on combined clinical and MRI features. *Frontiers in aging neuroscience*, *16*, 1414855.
26. Carey, G., et al. (2025). Reduced volume of the mediodorsal and anteroventral thalamus is associated with anxiety in Parkinson's disease: A cross-sectional 7-tesla MRI study. *J Parkinsons Dis*, *15*(2), 338–348.

27. Vriend, C., et al. (2016). A smaller amygdala is associated with anxiety in Parkinson's disease: a combined FreeSurfer-VBM study. *Journal Of Neurology, Neurosurgery And Psychiatry*, *87*(5), 493–500.
28. Yuan, J., et al. (2024). Alterations in cortical volume and complexity in Parkinson's disease with depression. *Cns Neuroscience & Therapeutics*, *30*(2), e14582.
29. Park, J., et al. (2020). An investigation of thalamic nuclei volumes and the intrinsic thalamic structural network based on motor subtype in drug naïve patients with Parkinson's disease. *Parkinsonism & Related Disorders*, *81*, 165–172.
30. Gibson, J. S., et al. (2023). Predictors of anxiety in Parkinson's disease: results from a 3-year longitudinal cohort study. *Neurological Sciences : Official Journal Of The Italian Neurological Society And Of The Italian Society Of Clinical Neurophysiology*, *44*(2), 547–556.
31. Jain, N., et al. (2023). It goes both ways: The relationship between anxiety and mild cognitive impairment. *International Journal Of Geriatric Psychiatry*, *38*(3), e5899.
32. van Griethuysen, J. J. M., et al. (2017). Computational Radiomics System to Decode the Radiographic Phenotype. *Cancer Research*, *77*(21), e104–e107.

# Figures

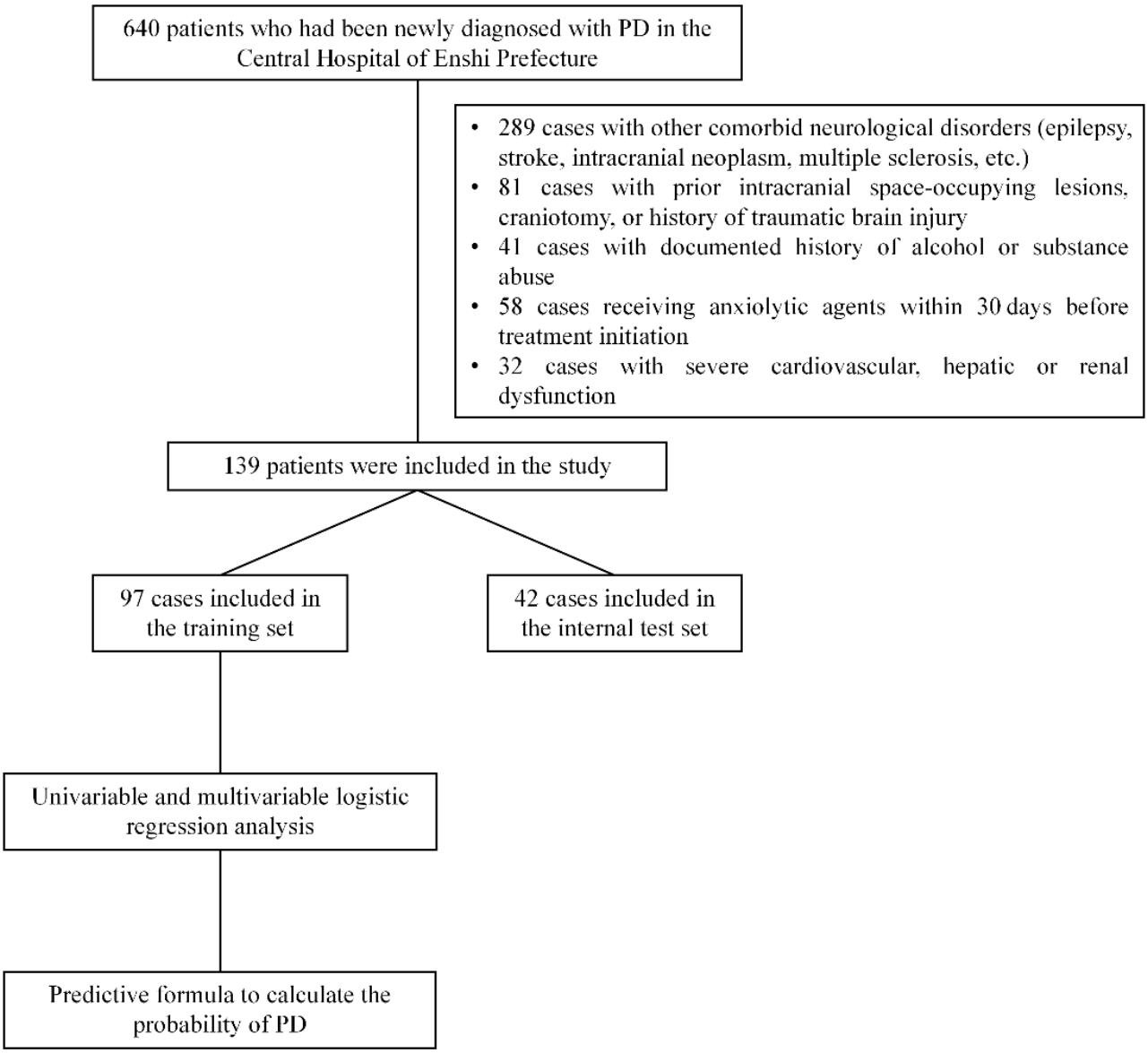



**Figure 1**

Flowchart of the study subjects based on exclusion criteria.

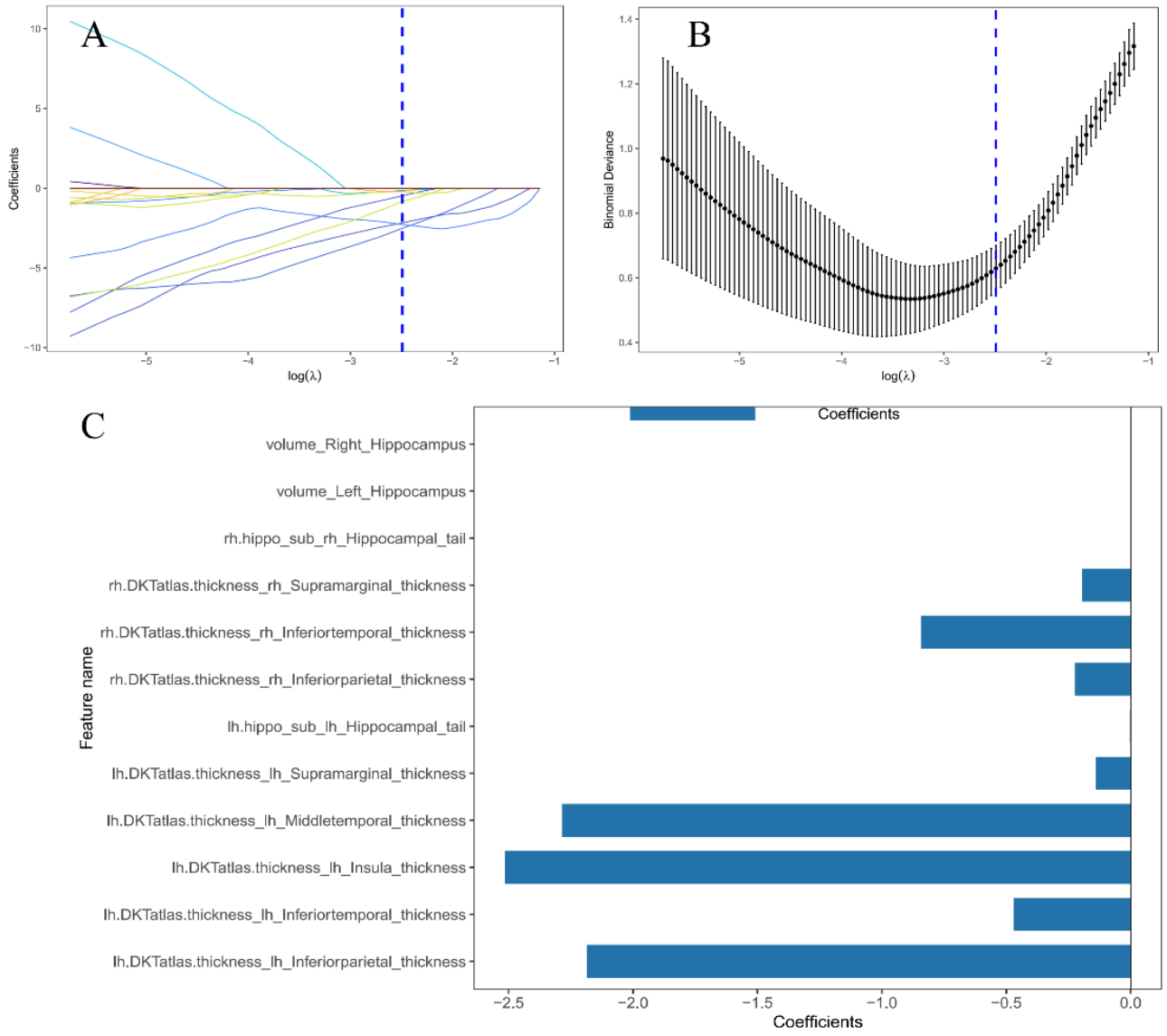
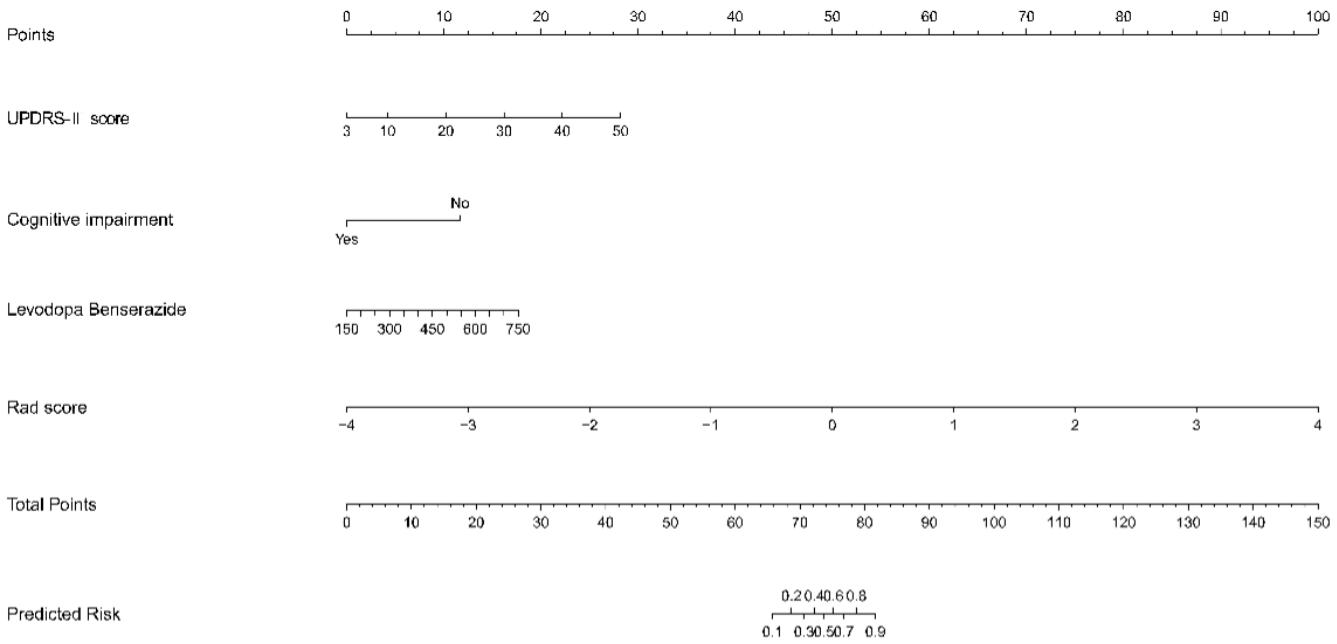



**Figure 2**

Radiomic feature extraction. (A, B) Radiomic features extraction using least absolute shrinkage and selection operator (LASSO) algorithm. (C) The final features included in our study.




## Figure 3

A nomogram integrates clinical parameters and radiomics features.

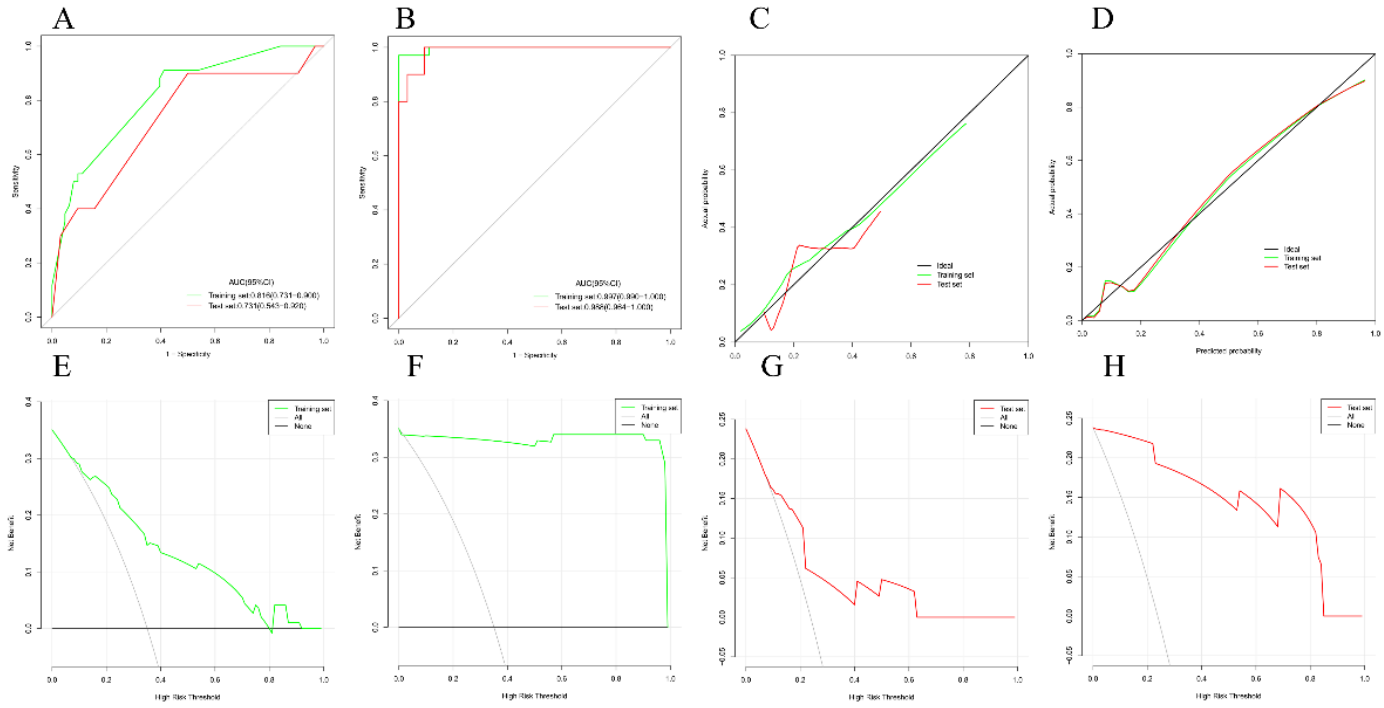


**Figure 4**

The performance of clinical model and combined nomogram with ROC, calibration curves and decision curve analysis. (A, B) ROC curves of each cohort in the (A) clinical model and (B) combined model for prediction of PDA. (C, D) Calibration curves of each cohort in the (C) clinical model and (D) combined model for prediction of PDA, and a 45° diagonal line indicates perfect calibration. (E, H) Decision curve analysis of each cohort in the (E, G) clinical model and (F, H) combined model for prediction of PDA, and the colored lines were expected net benefit of per patient. ROC, Receiver operating characteristics curves; PDA, PD with anxiety.

## Supplementary Files

This is a list of supplementary files associated with this preprint. Click to download.

- Appendix123.docx